H_2 Activation in Zeolites

DOI: 10.1002/anie.201201000

Unprecedented Reversible Redox Process in the ZnMFI—H_2 System Involving Formation of Stable Atomic Zn^0**

*Akira Oda, Hiroe Torigoe, Atsushi Itadani, Takahiro Ohkubo, Takashi Yumura, Hisayoshi Kobayashi, and Yasushige Kuroda**

Hydrogen activation is a key process in catalytic hydrogenation and hydrogen-transfer reactions. The study of the adsorption and activation of H_2 on solid materials is thus of great importance for research areas, such as H_2 activation on solid surfaces for applications in catalysis and vehicle fuel cells, as well as H_2 storage.[1] Zinc-ion-exchanged high-silica-type zeolites, such as the zinc-ion-exchanged MFI-type (ZnMFI) zeolite, are known to be efficient catalysts for the dehydrogenation and aromatization of light alkanes,[2] despite the Zn^{2+} ion, which has a d^{10} electronic configuration, being generally considered to have low reactivity. Therefore, an investigation of the surface properties of the Zn^{2+} ions that are incorporated into zeolites through exchange in the context of H–H bond activation is of importance because of the analogies with the C–H bond activation caused by the ZnMFI zeolite.[3–5] We wanted to clarify the roles of the Zn^{2+} ions within ZnMFI zeolites in H_2 activation. Herein, we describe the properties associated with the adsorption and activation of H_2 molecules in ZnMFI samples, properties, which were identified using experimental and theoretical methods. The results show that H_2 is activated at the Zn^{2+}-containing M7 sites of MFI-type zeolites with a specific environment.[6] A new and fascinating phenomenon was observed on this site: the Zn^{2+} ion was converted into a stable Zn^0 species through reaction with H_2 at 573 K, despite the order in the reduction potentials of Zn^{2+} ($E^0 = -0.762$ V) and H^+;[7] furthermore, the Zn^0 species undergoes reversion to the Zn^{2+} species upon heating the zeolite in vacuo.

IR spectroscopy was used to determine the identity of the species that is formed when the ZnMFI zeolite reacts with H_2 at 300 K. When the zeolite was exposed to H_2 (13.3 kPa) at 300 K, specific bands were observed at 3615 cm^{-1} and 1933 cm^{-1}; the bands were assigned to the OH stretching vibration associated with the Brønsted-acid site and the ZnH^+ stretching vibration, respectively, (see the Supporting Information, Figure SI-1), thus indicating heterolytic bond dissociation of H_2 at 300 K, a behavior, which was previously observed in the interaction between ZnO and H_2.[8] These IR bands were still observed after evacuation of the zeolite at 300 K, thus indicating that strongly adsorbed species are formed upon interaction with H_2 even at 300 K. These data are consistent with the isotherm data (Figure SI-2). Notably, only a small percentage (10–15%) of the incorporated zinc ions are responsible for the bond dissociation of H_2. H_2 adsorption on MgMFI(N)-82 zeolites (magnesium-ion-exchanged MFI-type zeolite wherein the number, 82, represents the percentage of sodium ions exchanged for magnesium ions during their preparation) was also investigated by using conditions similar to those used for ZnMFI(N)-95 zeolites (Figure S1-2).[9] It is clear from the data that H_2 barely adsorbed on MgMFI(N)-82 zeolites; similarly, H_2 did not adsorb on HMFI (hydrogen-ion-exchanged MFI-type) zeolites. These data clearly indicate that the particular electronic and structural states of the Zn^{2+} ions in ZnMFI zeolites plays a pivotal role in the heterolytic bond dissociation of H_2 with these zeolites at 300 K.

IR spectra show behavior characteristic of heterolytic bond dissociation of H_2 on ZnFMI zeolites at temperatures up to 573 K at a H_2 pressure of 13.3 kPa (Figure SI-1). The area of the IR band associated with the OH moiety increases with increasing temperatures; the IR band associated with the ZnH moiety also increases with increasing temperatures but attains a maximum area at treatment temperatures of approximately 423 K, and the area of the band subsequently decreases upon further increase in temperature. To examine this behavior, the area of the IR bands was plotted against treatment temperature (Figure 1). Below 423 K, bond dissociation of H_2 takes place heterolytically and with simultaneous formation of a zinc hydride and a Brønsted acid moiety [Eq. (1)], where Z_A and Z_B are lattice sites containing aluminum atoms. At temperatures higher than 423 K, the amount of the ZnH species decreases, despite an increase in the amount of the OH species. This behavior can be reasonably interpreted by assuming the formation of a Zn^0 species [Eq. (2)].

[*] A. Oda, H. Torigoe, Dr. A. Itadani, Dr. T. Ohkubo, Prof. Dr. Y. Kuroda
Department of Chemistry, Okayama University
3-1-1 Tsushima-naka, Kita-ku, Okayama 700-8530 (Japan)
E-mail: kuroda@cc.okayama-u.ac.jp
Dr. T. Yumura, Prof. Dr. H. Kobayashi
Department of Chemistry and Materials Technology
Kyoto Institute of Technology
Matsugasaki, Sakyo-ku, Kyoto 606-8585 (Japan)

[**] XAFS spectra were acquired under the proposal numbers of 2008G064, 2008G616, 2009G591, and 2011G538 of the Photon Factory Program Advisory Committee. We thank Prof. M. Nomura, Dr. H. Nitani, and Dr. A. Koyama of KEK in Tsukuba for their kind assistance in acquiring the XAFS spectra. Financial support was provided by the Ministry of Education, Culture, Sports, Science and Technology of Japan (No. 21655021). H.T. acknowledges financial support from Japan Society for the Promotion of Science (Research Fellowship for Young Scientists, DC1).

Supporting information, which includes details of sample preparation, the determination of ion-exchange level, spectroscopic data, and DFT calculations, for this article is available on the WWW under http://dx.doi.org/10.1002/anie.201201000.

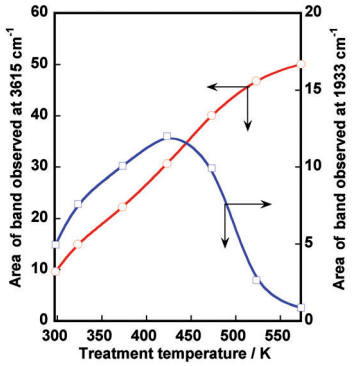

Figure 1. Intensity of IR bands, assigned to an OH species (circles) and a ZnH species (squares), of ZnMFI zeolites treated with H_2 at various temperatures. The intensity of the bands was normalized with reference to the band observed at 1892 cm^{-1}, which was assigned to the lattice mode of the zeolite.

$$Z_A{-}O{-}Zn^{2+}{-}O{-}Z_B + H_2 \rightarrow Z_A{-}O{-}(ZnH)^+ + Z_B{-}OH^+ \quad (1)$$

$$Z_A{-}O{-}(ZnH)^+ \rightarrow Zn^0 + Z_A{-}OH^+ \quad (2)$$

$$Z_A{-}O{-}Zn^{2+}{-}O{-}Z_B + H_2 \rightarrow Z_B{-}OH^+ + Zn^0 + Z_A{-}OH^+ \quad (\text{Total})$$

These data suggest that when ZnMFI zeolites are treated with H_2 at temperatures higher than 423 K, Zn^0 species are formed within the ZnMFI, via an intermediate cationic ZnH species; this result is inconsistent with the standard reduction potentials, that is, the ionization tendencies, of the species involved.[7]

On the basis of these experimental data, we investigated the heterolytic bond dissociation of H_2 through DFT calculations adopting models wherein two silicon atoms in the six-membered ring (6-MR) of the M7 site in the skeleton of the MFI lattice, were replaced with two aluminum atoms.[6] The resulting loss in positive charge would be compensated by the incorporation of a single Zn^{2+} ion; this type of model is based on previously reported work (these models, which exhibit different distances between the two aluminum atoms, are depicted in Figure SI-3).[6] In the models (Figure SI-3, S1–S4), the Zn^{2+} ion is situated close to the midpoint between the two aluminum atoms and is stabilized in the 6-MR by simultaneously compensating for the loss of positive charge resulting from the exchange of two silicon atoms for two aluminum atoms. In addition, EXAFS data (see the Supporting Information, Figure SI-4) related to the coordination number of the first shell observed in the spectrum, (*N* is approximately 3) are not in conflict with the present results; the zinc ion is surrounded by three oxygen atoms with bond lengths between 2.06 and 2.61 Å (Figures SI-3 and SI-4, and Table SI-1). Taking these points into consideration, we recognized four reasonable models that differ in the positions of the aluminum atoms in the M7 site (a detailed discussion of other models is given in the Supporting Information; Figure SI-5). Among the models for the M7 site, the S2 model works especially well as the site for bond dissociation of H_2. For this model, a number of structural changes, which occur without activation energy, were found upon bond dissociation of H_2. The position of the H_2 molecule changes from that of an end-on coordination to an η^2-like coordination; this is followed by continuous elongation of the bond between the two hydrogen atoms leading to complete bond dissociation of H_2, thus forming both ZnH and OH species (Figure 2). The IR bands of final species were calculated as 1922 cm^{-1} ($\nu_{Zn\text{-}H}$) and 3656 cm^{-1}

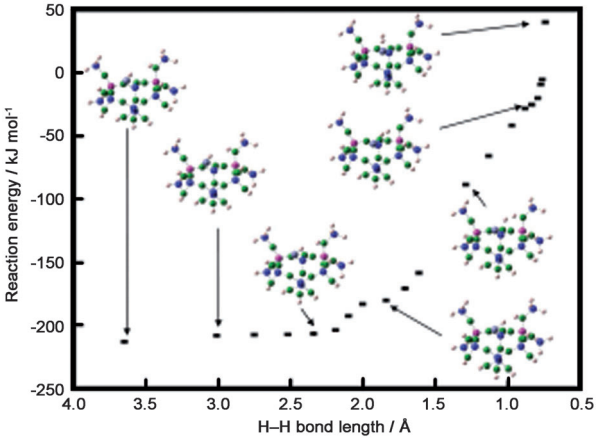

Figure 2. Reaction energies as a function of H–H bond distance, as calculated using DFT, for the reaction of H_2 with the Zn^{2+}-containing M7 site of MFI-type zeolites. Calculations were done on the S2 model of the M7 site, as given in the Supporting Information (Figure SI-3 and SI-6).

($\nu_{O\text{-}H}$) (Figure SI-6). In addition, the resulting reaction energy was calculated as −213 kJ mol^{-1}, and the distances between the hydrogen and zinc atoms, and between the hydrogen and oxygen atoms of the formed species were calculated as 1.51 Å (Zn–H1) and 0.97 Å (H2–O4), respectively (Figure SI-6). The evaluated adsorption energy corresponds well with the data on the bond energy for the Zn-H species reported by Platts;[10] the bond distance and IR data of the ZnH species (Figure SI-1 and Figure SI-6) are consistent with the data related to the ZnH species formed in the gas phase.[11] Prior to H_2 adsorption, the Zn^{2+} ion compensates the loss of positive charge that results when two silicon atoms are replaced by two aluminum atoms by being positioned at the midpoint between the resulting aluminum atoms; after bond dissociation of H_2, the zinc atom is at a position where it is still able to compensate for the loss of positive charge (Figure SI-6). Whether H_2 undergoes bond dissociation depends on the energy stabilization, which is in turn determined by the position of the zinc atom; there is a subtle balance in that the zinc atom should not be too far away yet not too close to the aluminum atoms. Notably, the reaction energy and IR band associated with the formed ZnH species is similar to that of the species in the 8-membered ring in MOR that was proposed by Pidko and van Santen, although the proposed model is different, the distant placing of two aluminum ions being termed Zn-Z_d.[12] It was calculated that H_2 could also undergo bond dissociation using the S3 model. However, the bond dissociation was not as favorable as that calculated for the S2 model, because the reaction energy was calculated to be −82 kJ mol^{-1} (Figure SI-7); additionally, the calculated IR

bands ($\nu_{Zn\text{-}H} = 1909\ cm^{-1}$ and $\nu_{O\text{-}H} = 3306\ cm^{-1}$) do not agree with those obtained by experiment. In addition, a viable pathway to H_2 bond dissociation was not found in calculations involving the S1 and S4 models (Figure SI-4).

Diffuse reflectance (DR) spectra of the ZnMFI(N)-95 zeolite treated with H_2 are given in Figure 3a. Prior to the measurement of spectra, the samples were treated in the following way: the zeolite was evacuated at 873 K; it was then treated at various temperatures in a H_2 atmosphere (13 kPa) for 0.5 hours; the sample was then cooled to 300 K without reevacuation and DR was measured. A sample that was evacuated at 873 K, but not subsequently exposed to a H_2 atmosphere (Figure 3a, spectrum 1), showed a weak band at around 39000 cm^{-1} (indicated by an arrow), which was assigned to the 3d–4s transition. When this sample was then treated with H_2 (13 kPa) at 300 K, the spectrum barely changed (Figure 3a, spectrum 2). A small change in the spectrum was observed when the sample was treated with H_2 at 373 K (Figure 3a, spectrum 3). Subsequent treatment at 473 K brought about the appearance of distinct bands at 42000 and 47000 cm^{-1} (Figure 3a, spectrum 5; bands indicated by arrows). These bands increase in intensity with increasing treatment temperature, and reached a maximum intensity at 573 K (Figure 3a, spectrum 7). Subsequent treatments at higher temperatures (as high as 773 K) with H_2 (13 kPa), caused no change in the spectra. Together with the IR data presented above, the strong bands observed in the DR spectra could be associated with the formation of atomic metal species or particles. Similar data was collected when the DR experiments were carried out under a lower pressure of H_2 (0.67 kPa).

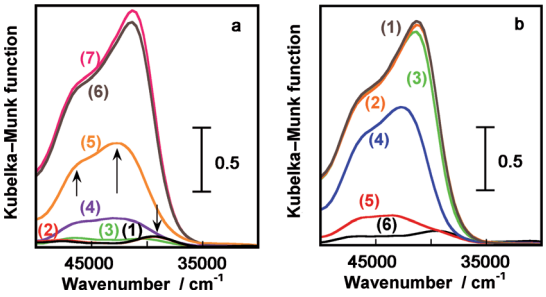

Figure 3. a) DR spectra of the ZnMFI zeolite in the reaction with H_2 at various temperatures: spectrum 1) ZnMFI(N)-95 zeolite evacuated at 873 K; spectra 2–7) ZnMFI(N)-95 zeolite evacuated at 873 K and then exposed to H_2 at 13 kPa at 300, 373, 423, 473, 523, and 573 K, respectively. b) DR spectra 1–6 of a ZnMFI(N)-95 zeolite evacuated at 873 K, then exposed to H_2 vapor at 13 kPa at 573 K (spectrum 7, Figure 3a), and then reevacuated at 300, 473, 573, 673, 773, and 873 K, respectively.

Zeolites that were treated with H_2 gas at temperatures of 573 K, or higher, as in the above experiment, were subsequently reevacuated at increasing temperatures from 300 to 873 K (Figure 3b). Reevacuation at temperatures between 300 and 573 K resulted in a small change in the strong DR bands at 42000 and 47000 cm^{-1} (Figure 3b, spectra 1 to 3). When the zeolite was reevacuation at 673 K, the furnished strong DR bands underwent a reduction in intensity to become DR bands of moderate intensity (Figure 3b, spectrum 4). After a subsequent treatment at 773 K (Figure 3b, spectrum 5), the DR bands had greatly decreased in intensity and the resultant spectrum was similar to that of the sample that was pretreated at 423 K with H_2. Reevacuation at 873 K resulted in a spectrum that was similar to that of the zeolite that was not exposed to H_2 gas (Figure 3a, spectrum 1 and Figure 3b, spectrum 6). These results, the DR spectra of zeolites that were treated with H_2 at various temperatures and that of zeolites that were subsequently reevacuated at various temperatures, clearly show the reversibility in the reaction between H_2 and the zeolite. When the zeolites used in the above experiments were resubjected to the H_2 treatment and reevacuation experiments, the same spectral behavior was observed, thus showing that the cycle is highly stable. Yates carried out pioneering research on the formation of Zn metal particles in the zinc-ion-exchanged X-type zeolite through treatment with H_2 at high temperatures.[13] The reaction conditions used in the work herein are far milder than those of Yates, and the formed metal species herein do not undergo further transformation during treatment with H_2 at the higher temperature of 773 K (not vaporize from the zeolite sample); furthermore, our observation that the Zn^{2+} species can be recovered through reevacuation of the zeolite is a completely new phenomenon.

To confirm the reversibility of the transformation of Zn^{2+} into Zn^0, we carried out the following experiment: the ZnMFI(N)-95 zeolite was first evacuated at 873 K and then H_2 adsorption was measured as a function of H_2 pressure at 573 K (isotherm 1, Figure SI-8); the zeolite was then reevacuated at 573 K and H_2 adsorption was measured again as a function of H_2 pressure at 573 K (isotherm 2, Figure SI-8); the last step was repeated using different evacuation temperatures, 673, 773, and 873 K, to give isotherms 3, 4, and 5, respectively (see also Table SI-2). These data also show that when ZnMFI(N)-95 zeolites that were treated with H_2 are reevacuated at 873 K, they revert to the state they were in prior to H_2 treatment. This reaction at 873 K, the reversion of species that were initially formed according to reactions (1) and (2) can be written as [Eq. (3)]. All of the processes, including those represented by Eqs. (1)–(3), are schematically represented in the Supporting Information, Figure SI-9.

$$Zn^0 + Z_A{-}OH^+ + Z_B{-}OH^+ \rightarrow Z_A{-}O{-}Zn^{2+}{-}O{-}Z_B + H_2\uparrow \qquad (3)$$

As described above, the DR spectra are consistent with the formation of a Zn^0 species upon treatment of the ZnMFI zeolite with H_2 at temperatures higher than 423 K. The formation of Zn^0 species and its conversion back into Zn^{2+}, which was achieved through reevacuation of the zeolite at 873 K, could be repeated again and again, thus representing a complete redox cycle. We performed time-dependent (TD) DFT calculations on a single Zn atom, as well as on a composite of two atoms, to determine whether we could theoretically reproduce the experimentally obtained DR spectra (Figure 4).

First, we confirmed that the spectrum of the sample treated at 873 K (spectrum 1, Figure 4) represents a Zn^{2+}

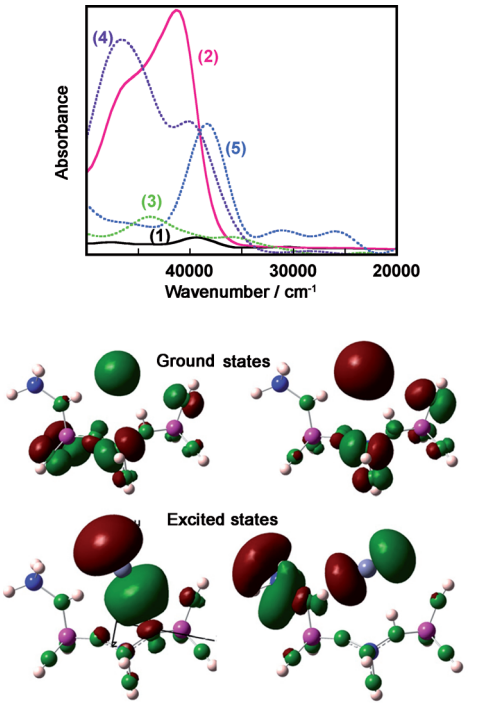

Figure 4. Absorption spectra obtained experimentally (solid lines) and with the aid of TD-DFT calculations (dashed lines): spectrum 1) ZnMFI(N)-95 sample evacuated at 873 K; spectrum 2) ZnMFI(N)-95 sample treated with H_2 at 573 K; spectrum 3) TD-DFT calculated spectrum of Zn^{2+}-containing M7 site of the S2 model; spectrum 4) TD-DFT calculated spectrum of a single Zn^0 species interacting with two OH groups; spectrum 5) TD-DFT calculated spectrum of a dimeric Zn^0 species interacting with OH groups. The positions of all elemental metal and metal ions in the sites were optimized prior to the TD-DFT calculation. The ground and excited states of the monomeric Zn^0 species are also shown.

species by comparing it with the theoretically derived spectrum (spectrum 3, Figure 4). We assumed that when the Zn^0 species is formed, according to the model proposed above, two H^+ ions are formed as constituents of two Brønsted acid sites, OH species, which compensate for the replacement of two silicon ions for two aluminum ions. We then carried out DFT calculations using a larger model that better represented the pore structure in the zeolite.[6] These calculations showed that the Zn^0 species is stable and is favorably located close to the formed OH species in the pore (Figure SI-10a). A subsection of the model that included the Zn^0 species was truncated from the larger model and reoptimized (Figure SI-10b). A TD-DFT calculation was carried out on this optimized substructure to obtain a theoretical DR spectrum. For comparison, a similar treatment was carried out on a dimeric model (Figure SI-10c). The calculated DR spectrum for the optimized substructure (Figure 4, spectrum 4), wherein a single Zn^0 species is represented by strong bands centered at around 46500 and 40000 cm^{-1}, compared well with the experimentally obtained DR spectrum, which exhibits peaks at around 45600 and 41350 cm^{-1} (Figure 4, spectrum 2). These peaks can be attributed to the 4s–4p electronic transition of a Zn^0 species; representations of the ground and excited states associated with the electronic transition are given in Figure 4. On the other hand, calculations on the dimeric model gave spectrum 5. These results allow us to conclude that when a ZnMFI zeolite is treated with H_2 at high temperatures, a Zn^0 species is formed via ZnH and OH species (Figure SI-9); this is the first example of such a phenomenon. A similar formation of anchored single elemental atoms in HY-type zeolites that had undergone metal exchange with $[Ir(C_2H_4)_2(acac)]$ (acac = acetyl acetonate) has been demonstrated by the (HAADF)STEM method.[14]

To add further support to the claim that Zn^0 species are formed when ZnMFI zeolites are treated with H_2 at high temperature, we acquired XANES spectra of ZnMFI zeolites that were treated with H_2 at both 473 and 573 K, followed by evacuation at higher temperatures (Figure 5; for comparison,

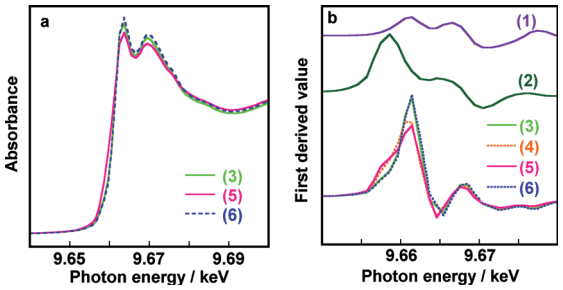

Figure 5. a) XANES spectra and b) DXANES spectra: spectrum 1) ZnO reference sample; spectrum 2) Zn reference sample; spectra 3) ZnMFI(N)-95 zeolite evacuated at 873 K; spectrum 4) ZnMFI(N)-95 zeolite treated with H_2 at 473 K; spectra 5) ZnMFI(N)-95 zeolite treated with H_2 at 573 K, spectra 6) ZnMFI(N)-95 zeolite treated with H_2 at 573 K followed by reevacuation at 873 K. All measurements were performed at 300 K.

the spectra of reference samples are given in Figure SI-11).[15] When the ZnMFI zeolite was treated with H_2 at various temperatures, the resulting changes in the XANES spectra was very small. When the spectra of samples treated with H_2 at 473 and 573 K were examined in detail, a shoulder band appears at the lower energy side of the first main band (Figure 5a). We thus obtained the derivative of each XANES spectrum (abbreviated as DXANES) so that the changes in corresponding XANES spectra could be more easily visualized (Figure 5b). The DXANES spectra clearly show that a shoulder has appeared in the corresponding XANES spectra at around 9.658 keV; the Zn^0 reference sample gives a distinctive band at 9.659 keV in its DXANES spectrum. Notably, the intensity of the bands in this region of the spectrum of the sample that was treated with H_2 at 573 K is higher than those of the Zn^{2+}-exchanged samples (Figure 5b). The region of the DXANES spectrum centered at 9.658 keV of the H_2-treated sample agrees well with that of the Zn^0 reference sample. Mihelič et al. reported the XANES spectrum of atomic zinc vapor; the highest band of the spectrum was centered at approximately 9.66 keV;[15] this previously reported spectrum of Zn^0 strongly supports our assignment of the XANES band at 9.658 keV in our sample, despite the presence of only 10–15% of Zn^0. This band decreased in

intensity when the sample was evacuated at temperatures higher than 673 K and ultimately returned to an intensity that corresponded to that of the original sample, that is, the sample that was evacuated at 873 K and not treated with H_2. These results further support the existence of the reversible redox cycle, $Zn^{2+} \rightarrow ZnH \rightarrow Zn^0 \rightarrow Zn^{2+}$.

In summary, we examined H_2 activation in ZnMFI zeolites and demonstrated that a Zn^{2+} ion, introduced through exchange, at the M7 site of an MFI-type zeolite activates H_2. A new and fascinating phenomenon was found to occur at this M7 site: a stable Zn^0 species is formed through the reaction of Zn^{2+} with H_2 at 573 K, despite the order of the ionization tendency of Zn^{2+} ($E^0 = -0.762$ V) and H^+. DFT calculations provided evidence that the formed species is composed of an atomic Zn^0 stabilized through simultaneous interaction with two H^+ ions at Brønsted acid sites; the Zn^0 species returned to its original state, the Zn^{2+} species, upon subjection to high temperature, thus establishing a redox cycle. This interpretation of the data was supported by DR spectra and XANES data. Successive H_2 treatment and evacuation at high temperature showed that the redox cycle, $Zn^{2+} \rightarrow ZnH \rightarrow Zn^0 \rightarrow Zn^{2+}$, was highly stable. The unusual and unprecedented features associated with the treatment of ZnMFI zeolites with H_2 were not observed for MgMFI zeolites.

Received: February 7, 2012
Revised: May 11, 2012
Published online: June 22, 2012

Keywords: density functional calculations · hydrides · hydrogen activation · redox chemistry · zeolites

[1] a) W. T. Josse, M. B. Hall in *Activation of Small Molecules* (Ed.: W. B. Tolman), Wiley-VCH, Weinheim, **2006**, pp. 121 – 150; b) W. Curtis Conner, Jr., J. L. Falconet, *Chem. Rev.* **1995**, *95*, 759 – 788; c) L. Wang, R. T. Yang, *Energy Environ. Sci.* **2008**, *1*, 268 – 279; d) U. Eberle, M. Felderhoff, F. Schüth, *Angew. Chem.* **2009**, *121*, 6732 – 6757; *Angew. Chem. Int. Ed.* **2009**, *48*, 6608 – 6630; e) P. Jena, *J. Phys. Chem. Lett.* **2011**, *2*, 206 – 211; f) S. F. Parker, *Faraday Discuss.* **2011**, *151*, 9 and other papers in this volume.

[2] a) T. Mole, J. R. Anderson, G. Creer, *Appl. Catal.* **1985**, *17*, 141 – 154; b) Y. Ono, *Catal. Rev. Sci. Eng.* **1992**, *34*, 179 – 226; c) J. A. Biscardi, E. Igresia, *Catal. Today* **1996**, *31*, 207 – 231; d) J. A. Biscardi, G. D. Meitzner, E. Iglesia, *J. Catal.* **1998**, *179*, 192 – 202; e) L. Li, G.-D. Li, C. Yan, X.-Y. Mu, X.-L. Pan, X.-X. Zou, K.-X. Wang, J.-S. Chen, *Angew. Chem.* **2011**, *123*, 8449 – 8453; *Angew. Chem. Int. Ed.* **2011**, *50*, 8299 – 8303.

[3] a) V. B. Kazansky, V. Y. Borovkov, A. I. Serikh, R. A. van Santen, B. G. Anderson, *Catal. Lett.* **2000**, *66*, 39 – 47; b) V. B. Kazansky, A. I. Serikh, B. G. Anderson, R. A. van Santen, *Catal. Lett.* **2003**, *88*, 211 – 217; c) A. A. Shubin, G. M. Zhidomirov, V. B. Kazansky, R. A. van Santen, *Catal. Lett.* **2003**, *90*, 137 – 142; d) V. B. Kazansky, A. I. Serykh, E. A. Pidko, *J. Catal.* **2004**, *225*, 369 – 373; e) V. B. Kazansky, E. A. Pidko, *J. Phys. Chem. B* **2005**, *109*, 2103 – 2108; f) I. R. Subbotina, V. B. Kazansky, J. Kröhnert, F. C. Jentoft, *J. Phys. Chem. A* **2009**, *113*, 839 – 844.

[4] a) Y. G. Kolyagin, V. V. Ordomsky, Y. Z. Khimyak, A. I. Rebrov, F. Fajula, I. I. Ivanova, *J. Catal.* **2006**, *238*, 122 – 133; b) A. G. Stepanov, S. S. Arzumanov, A. A. Gabrienko, V. N. Parmon, I. I. Ivanova, D. Freude, *ChemPhysChem* **2008**, *9*, 2559 – 2563; c) Y. G. Kolyagin, I. I. Ivanova, V. V. Ordomsky, A. Gedeon, Y. A. Pirogov, *J. Phys. Chem. C* **2008**, *112*, 20065 – 20069.

[5] a) A. G. Stepanov, S. S. Arzumanov, A. A. Gabrienko, A. V. Toktarev, V. N. Parmon, D. Freude, *J. Catal.* **2008**, *253*, 11 – 21; b) J. F. Wu, W. D. Wang, J. Xu, F. Deng, W. Wang, *Chem. Eur. J.* **2010**, *16*, 14016 – 14025; c) El-M. El-Malki, R. A. van Santen, W. M. H. Sachtler, *J. Phys. Chem. B* **1999**, *103*, 4611 – 4622; d) L. A. M. M. Barbosa, R. A. van Santen, *J. Phys. Chem. B* **2003**, *107*, 14342 – 14349; e) L. A. M. M. Barbosa, R. A. van Santen, *J. Phys. Chem. C* **2007**, *111*, 8337 – 8348; f) *Catalysis by Unique Metal Ion Structures in Solid Matrices* (Eds.: G. Centi, B. Wichterlova, A. T. Bell), Kluwer, Dordrecht, **2001**, pp. 55 – 73 & pp. 187 – 204; g) J. Penzien, A. Abraham, J. A. van Bokhoven, A. Jentys, T. E. Müller, C. Sievers, J. A. Lercher, *J. Phys. Chem. B* **2004**, *108*, 4116 – 4126.

[6] a) D. Nachtigallová, P. Nachtigall, M. Sierka, J. Sauer, *Phys. Chem. Chem. Phys.* **1999**, *1*, 2019 – 2026; b) T. Yumura, M. Takeuchi, H. Kobayashi, Y. Kuroda, *Inorg. Chem.* **2009**, *48*, 508 – 517; c) T. Yumura, H. Yamashita, H. Torigoe, H. Kobayashi, Y. Kuroda, *Phys. Chem. Chem. Phys.* **2010**, *12*, 2392 – 2400; d) H. Torigoe, T. Mori, K. Fujie, T. Ohkubo, A. Itadani, K. Gotoh, H. Ishida, H. Yamashita, T. Yumura, H. Kobayashi, Y. Kuroda, *J. Phys. Chem. Lett.* **2010**, *1*, 2642 – 2650.

[7] P. Atkins, T. Overton, J. Rourke, M. Weller, F. Armstrong, in *Inorganic Chemistry*, *4th ed.*, Oxford University Press, Oxford, **2006**.

[8] R. J. Kokes, *Acc. Chem. Res.* **1973**, *6*, 226 – 233.

[9] a) S. Aldridge, A. J. Downs, *Chem. Rev.* **2001**, *101*, 3305 – 3365; b) E. N. Gribov, S. Bertarione, D. Scarano, C. Lamberti, G. Spoto, A. Zecchina, *J. Phys. Chem. B* **2004**, *108*, 16174 – 16186.

[10] J. A. Platts, *J. Mol. Struct. (THEOCHEM)* **2001**, *545*, 111 – 118.

[11] a) T. M. Greene, W. Brown, L. Andrews, A. J. Downs, G. V. Chertihin, N. Runeberg, P. Pyykkö, *J. Phys. Chem.* **1995**, *99*, 7925 – 7934; b) A. Shayesteh, D. R. T. Appadoo, I. E. Gordon, P. F. Bernath, *J. Am. Chem. Soc.* **2004**, *126*, 14356 – 14357; c) X. Wang, L. Andrews, *J. Phys. Chem. A* **2004**, *108*, 11006 – 11013; d) A. Shayesteh, S. Yu, P. F. Bernath, *Chem. Eur. J.* **2005**, *11*, 4709 – 4712.

[12] E. A. Pidko, R. A. van Santen, *J. Phys. Chem. C* **2007**, *111*, 2643 – 2655.

[13] D. J. C. Yates, *J. Phys. Chem.* **1965**, *69*, 1676 – 1683.

[14] V. Ortalan, A. Uzun, B. C. Gates, N. D. Browning, *Nat. Nanotechnol.* **2010**, *5*, 506 – 510.

[15] a) J. A. Biscardi, E. Iglesia, *Phys. Chem. Chem. Phys.* **1999**, *1*, 5753 – 5759; b) D. Grandjean, V. Pelipenko, E. D. Batyrev, J. C. van den Heuvel, A. A. Khassin, T. M. Yurieva, B. M. Weckhuysen, *J. Phys. Chem. C* **2011**, *115*, 20175 – 20191; c) A. Mihelič, A. Kodre, I. Arčon, J. Padežnik Gomilšek, M. Borowski, *Nucl. Instrum. Methods Phys. Res. Sect. B* **2002**, *196*, 194 – 197.

